



CHAPTER IV RESULTS AND DISCUSSIONS

4.1 Characterization of zinc waste

4.1.1 Phase analysis

X - ray diffraction pattern of zinc waste was observed as shown in Fig 4.1. Phase compositions of zinc waste were composed of Quartz (SiO_2), Anhydrite (CaSO_4), Cristobalite (SiO_2), Willemite (Zn_2SiO_4) and Magnetite (Fe_2O_3).

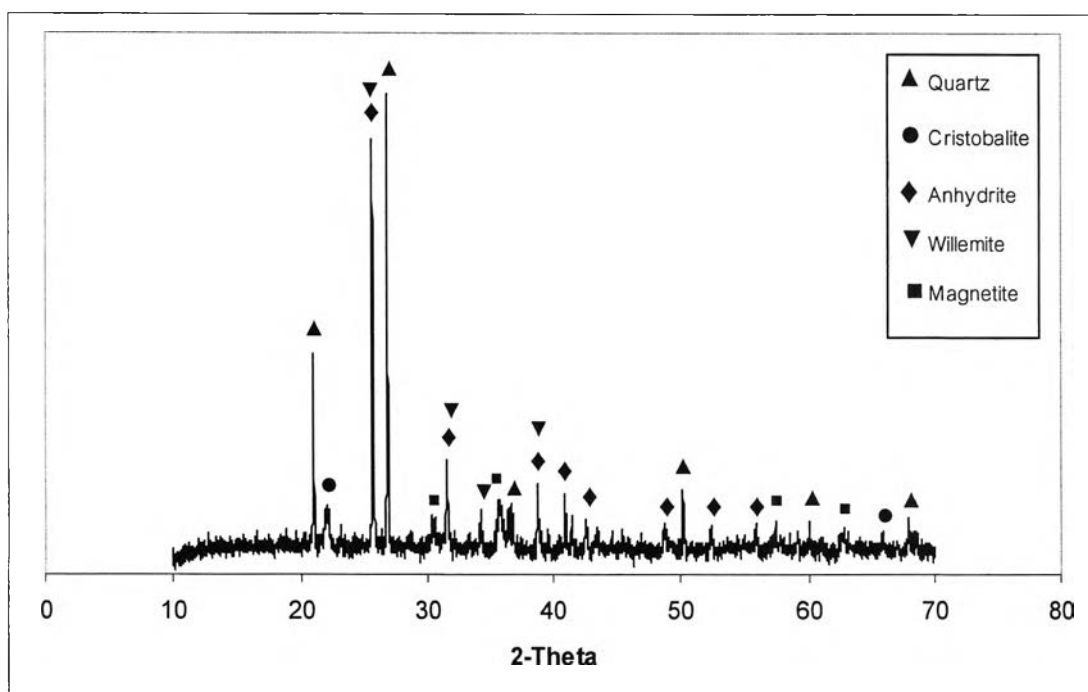


Fig 4.1 XRD pattern of zinc waste

4.1.2 Chemical composition

Chemical compositions of zinc waste in weight percent were shown in Table 4.1. There were various types of oxides contained in zinc waste, which were the by product of zinc hydrometallurgical process. Zinc waste was composed of SiO_2 (57.092 wt%) as major oxide. Minor oxides such as CaO (10.250 wt%), ZnO (9.534 wt%), Fe_2O_3 (7.546 wt%), Al_2O_3 (4.091 wt%) and SO_3 (4.813 wt%) were also observed. It was believed that CaO was originated from limestone which was used for natural leaching process.

SiO₂ and SO₃ came from silicate and sulfuric acid (H₂SO₄) used in leaching process, respectively; whereas others minor oxides were originated from leaching process and precipitation process [30].

Table 4.1 Chemical compositions of zinc waste

Oxides	(wt%)	Oxides	(wt%)
SiO ₂	57.09	ZnO	9.53
Al ₂ O ₃	4.09	SO ₃	4.81
Na ₂ O	0.01	PbO	1.23
MgO	1.19	TiO ₂	0.19
K ₂ O	0.83	P ₂ O ₅	0.10
CaO	10.25	MnO	0.54
Fe ₂ O ₃	7.55	CuO	0.17
L.O.I.(%)			2.42

4.1.3 Particle size distribution

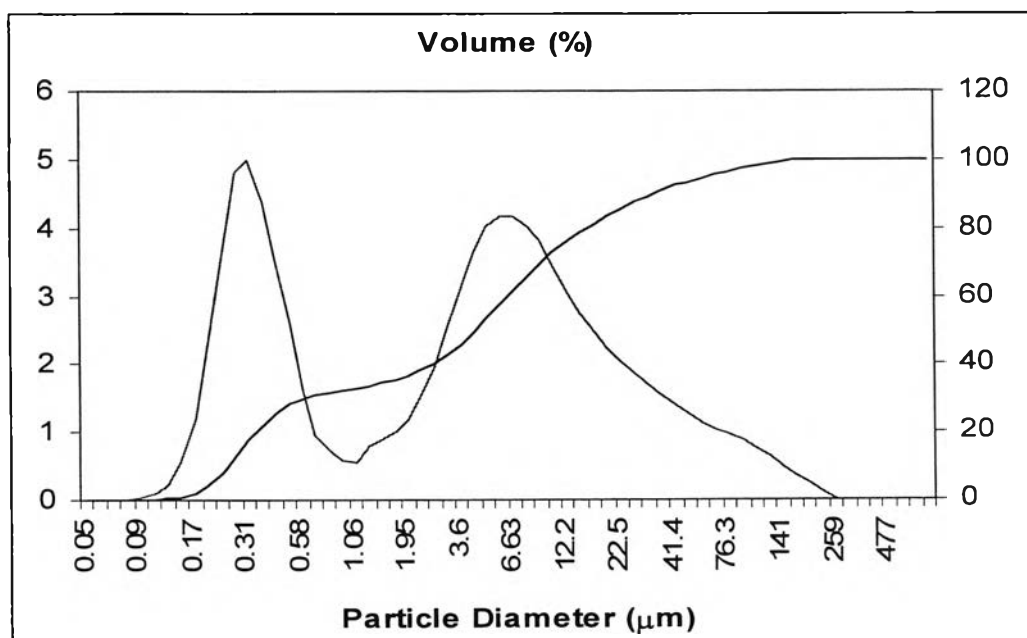


Fig 4.2 Particle size distribution of zinc waste

Particle size distribution of zinc waste was examined and shown in Fig 4.2. There were two peaks of particle size distribution curve. The first one was observed between 0.17 - 0.58 μm and the second one was between 2.65 - 26.2 μm . These indicated the containing of bimodal particle sizes distribution in this waste.

4.2 Characterization of tile bodies and glazes

4.2.1 Characterization of tile bodies

4.2.1.1 Physical properties

The physical properties of specimens after firing at temperature range from 1075°C-1175°C were observed.

- Visual observation

The color, shape and surface of specimens were changed after firing at different temperature as shown in Fig 4.3.

The color of the fired specimen was found to be dependent on both composition and firing temperature. At any selected firing temperature, the color shades of the tiles changed from brown to dark brown. The darkness of specimen increased from T1 to T11. That is the color was darker in specimen containing higher percentage of zinc waste. The change of color depended on the amount of zinc waste - higher percentage of the zinc waste, provided darker shade of tile color. At the same composition, the color shade of the specimens depended on the firing temperature. An increase in firing temperature resulted in darker color.

As the percentage of zinc waste increased, percent of Fe_2O_3 increased. The higher percentage of Fe_2O_3 , the darker colors of the specimens were. The change of color depends on weight percent of Fe_2O_3 .

Considering to the shape of specimens and the firing temperature, there was no shape distortion observed in all the specimens at firing temperatures up to 1125°C. However, after firing at 1150°C, the bloating was observed in specimens T5, T6, T7, T8, T9 and T10 and T11, which possessed high content ($\geq 40\%$) of zinc waste














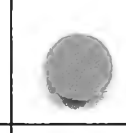
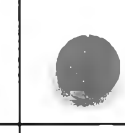


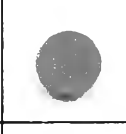






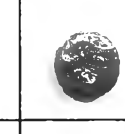




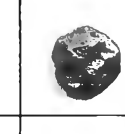




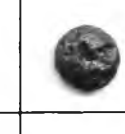




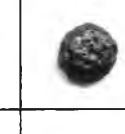









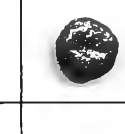




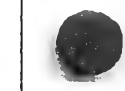
Specimens	Temperature				
	1075°C	1100°C	1125°C	1150°C	1175°C
T1					
T2					
T3					
T4					
T5					
T6					
T7					
T8					
T9					
T10					
T11					

Fig 4.3 Specimens after firing at various temperatures

According to phase and chemical composition of zinc waste, showed high quantity of CaSO_4 and SO_3 . At 1200°C , CaSO_4 decomposed to be CaO and SO_3 . This reaction happened up to 1325°C . This range of temperature was above the firing temperature of specimens. Decomposition occurs after vitrification had started; high pressure of gas from decomposition causes the bloating phenomena [31, 32, 33].

- Linear shrinkage and Bulk density

The linear shrinkage and bulk density of specimens were shown in Fig 4.4. and Fig 4.5, respectively.

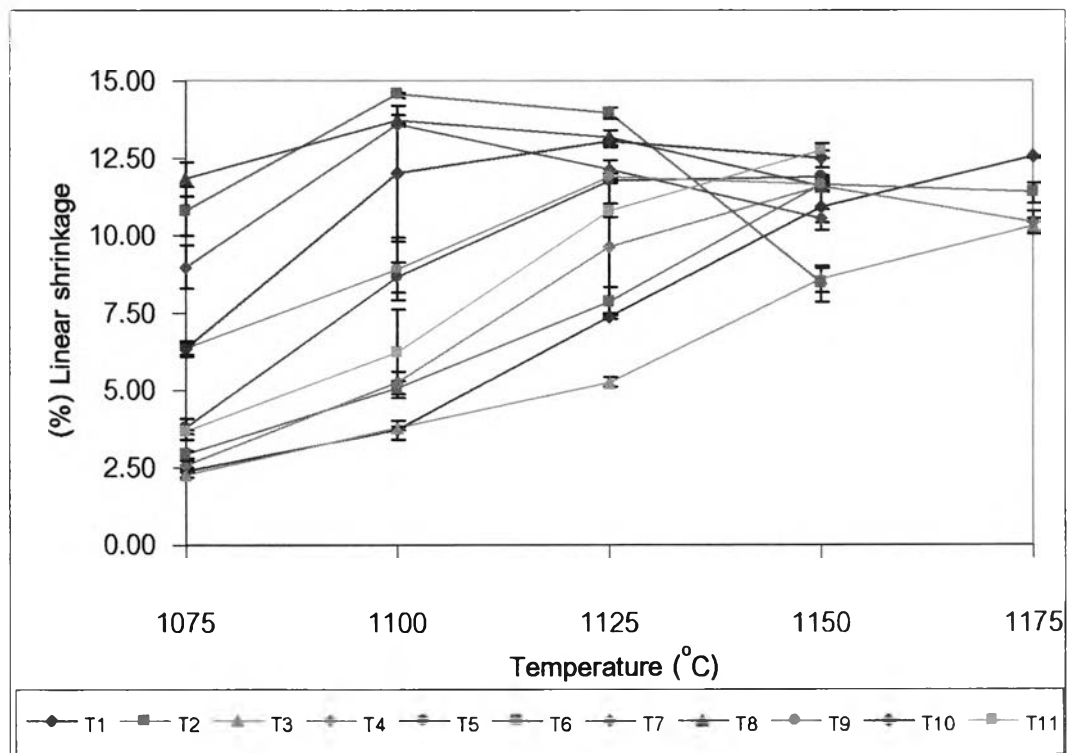


Fig 4.4 Percent linear shrinkage of specimens

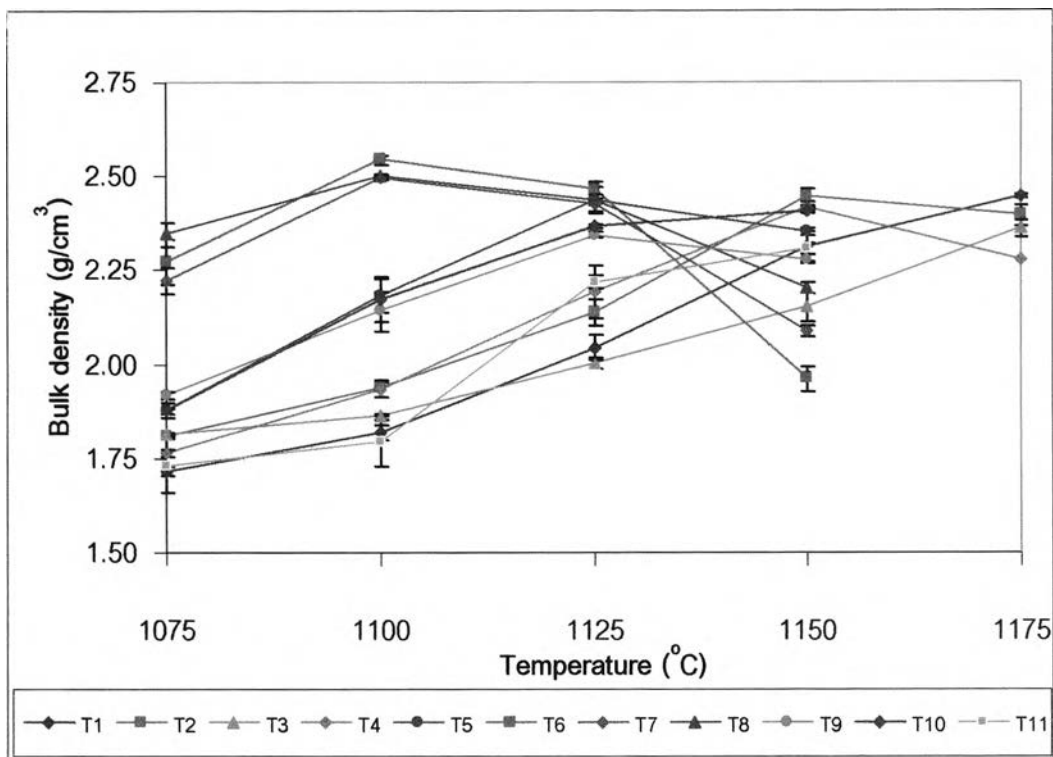


Fig 4.5 Bulk density of specimens

Linear shrinkage and bulk density of specimens T1, T2, T3, T4, T5, T10 and T11 increased with increasing temperature. For specimens T6, T7 and T8, their linear shrinkage increased up to 1100°C. Above this temperature, linear shrinkage decreased with increasing temperature. Specimen T9, linear shrinkage increased as a function of temperature up to 1125°C but as further increasing temperature, linear shrinkage decreased again.

The linear shrinkage of specimens was in range of 2.26-14.55 %. And bulk density of specimens was in range of 1.72-2.54 g/cm³.

At maximum linear shrinkage and bulk density of several specimens, they were matured. Above this, linear shrinkage and bulk density decreased because of overfiring.

- Water absorption and apparent porosity

Fig 4.6 and Fig 4.7 show percent water absorption and percent apparent

porosity of specimens, respectively. Percent water absorption and percent apparent porosity of specimens T1, T2, T3, T4, T10 (1100 – 1150 °C), T5 and T9 (1100 – 1125 °C) decreased as firing temperatures increased. For specimens T5 and T9 after 1125 °C their water absorption slightly increased. Specimens T6, T7 and T8 obtained zero absorption when fired at as low as 1100 °C, increasing firing temperatures caused water absorption to increase due to overfiring and bloating of specimens. Higher percentages of zinc waste in specimens yielded lower water absorption at lower firing temperature. Water absorption of T6, T7 and T8 were obtained to zero at 1100°C. While, water absorption of T1,T2, T3, T4 and T5 were obtained to zero at higher temperatures. These all results were supported by linear shrinkage and bulk density of specimens.

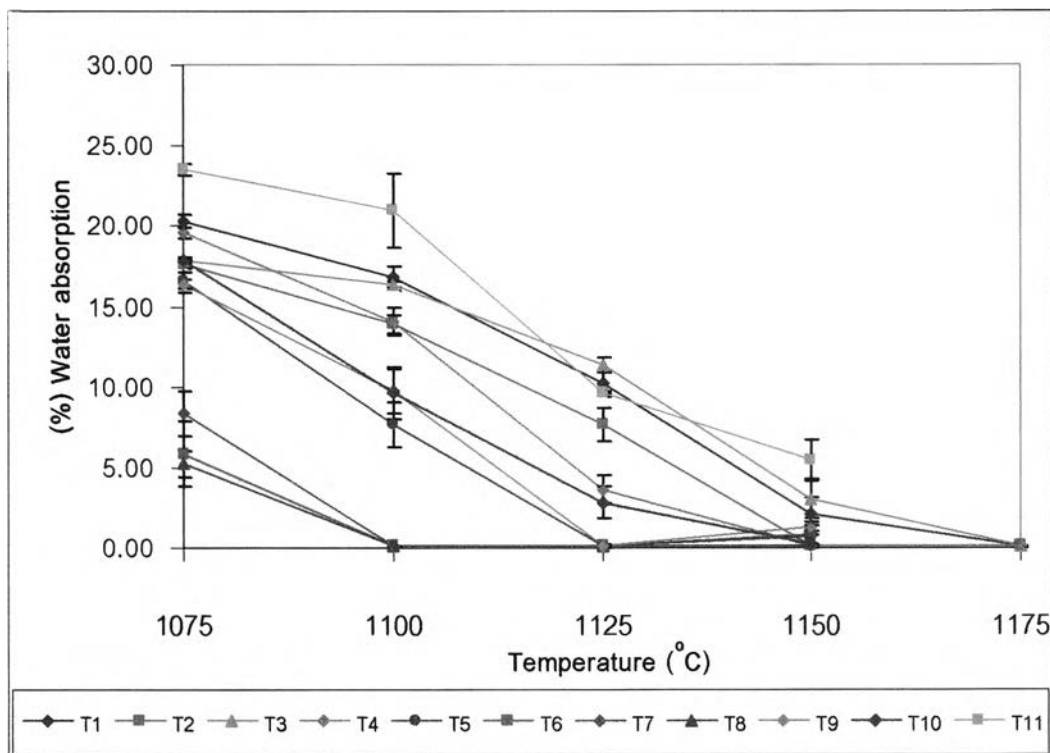


Fig 4.6 Percent water absorption of specimens

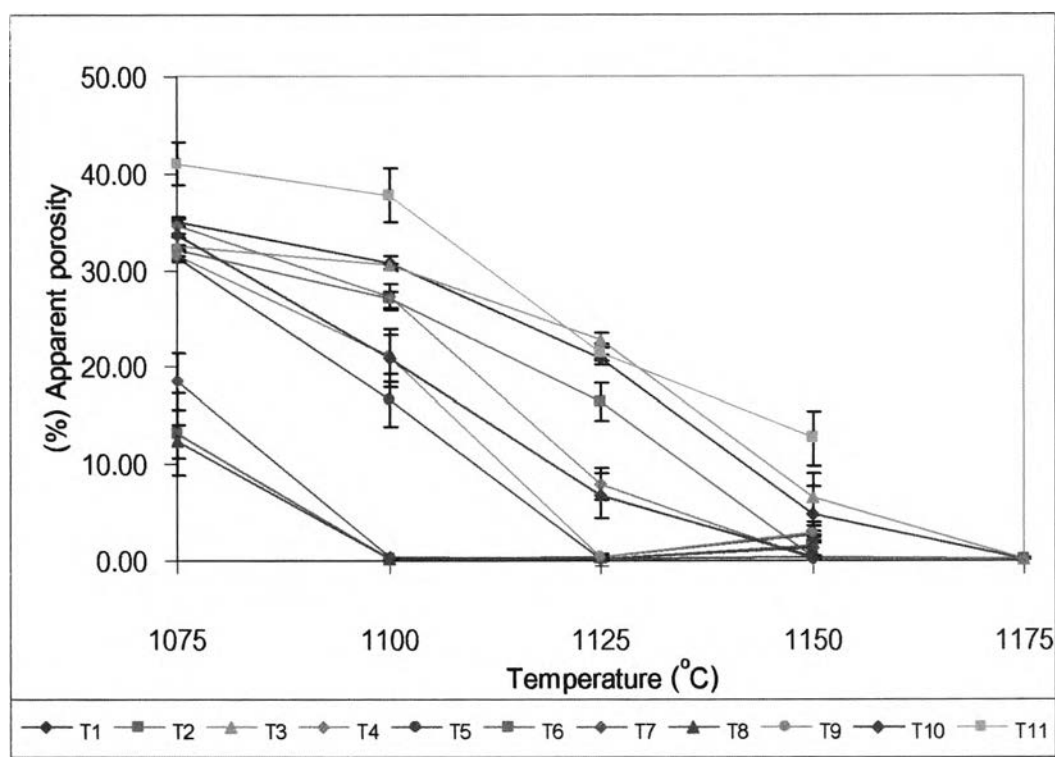


Fig 4.7 Percent apparent porosity of specimens

Percent water absorption and percent apparent porosity indicates the percent of open pores-those pores connected to the surface. During firing process some of open pores became closed pores. As the result, volume fraction of closed pore increased. Overfiring process some of closed pore became open pores, this lead to percent water absorption and percent apparent porosity increased. [34].

Due to zinc waste contained many of auxiliary fluxes such as CaO, Na₂O, MgO and ZnO, physical properties of specimens changed dramatically while the firing temperature changed for only 25°C. This indicated that some of these compositions had a very short firing range. In a real production, longer firing range was more desirable because it would be more flexible for change of firing temperature due to an unexpected circumstance.

According to DIN standard, water absorption of unglazed floor tile was not over than 5%. Therefore, fired specimens that were no shape distortion and water absorption lower than 5%, i.e. specimens T1, T4, T5, T6, T7 and T8, were selected to examine phases, strength and chemical properties.

4.2.1.2 Microstructure

Fig 4.8 shows OM images of specimen T6, T7 and T8 after firing at 1100°C. The samples were cross-sectioned and then polished.

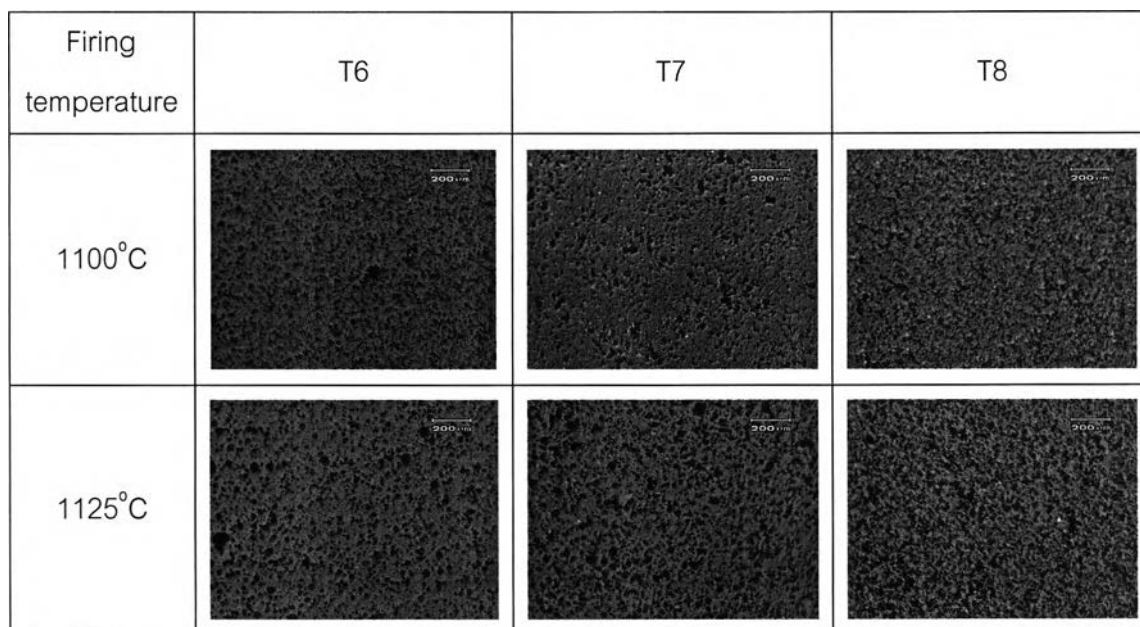


Fig 4.8 Microstructure of cross-section of specimens T6, T7 and T8 fired at 1100°C and 1125°C.

All specimens consisted mainly of fine pores. These pores connected and became larger after firing at higher temperature (1125°C). This indicates that the specimens began to be overfired or bloating. This result was confirmed by linear shrinkage, bulk density, water absorption and apparent porosity of the specimens.

4.2.1.3 Phase formation analysis

Phase formations of selected specimens fired at 1125°C were analyzed by XRD as shown in Fig 4.9.

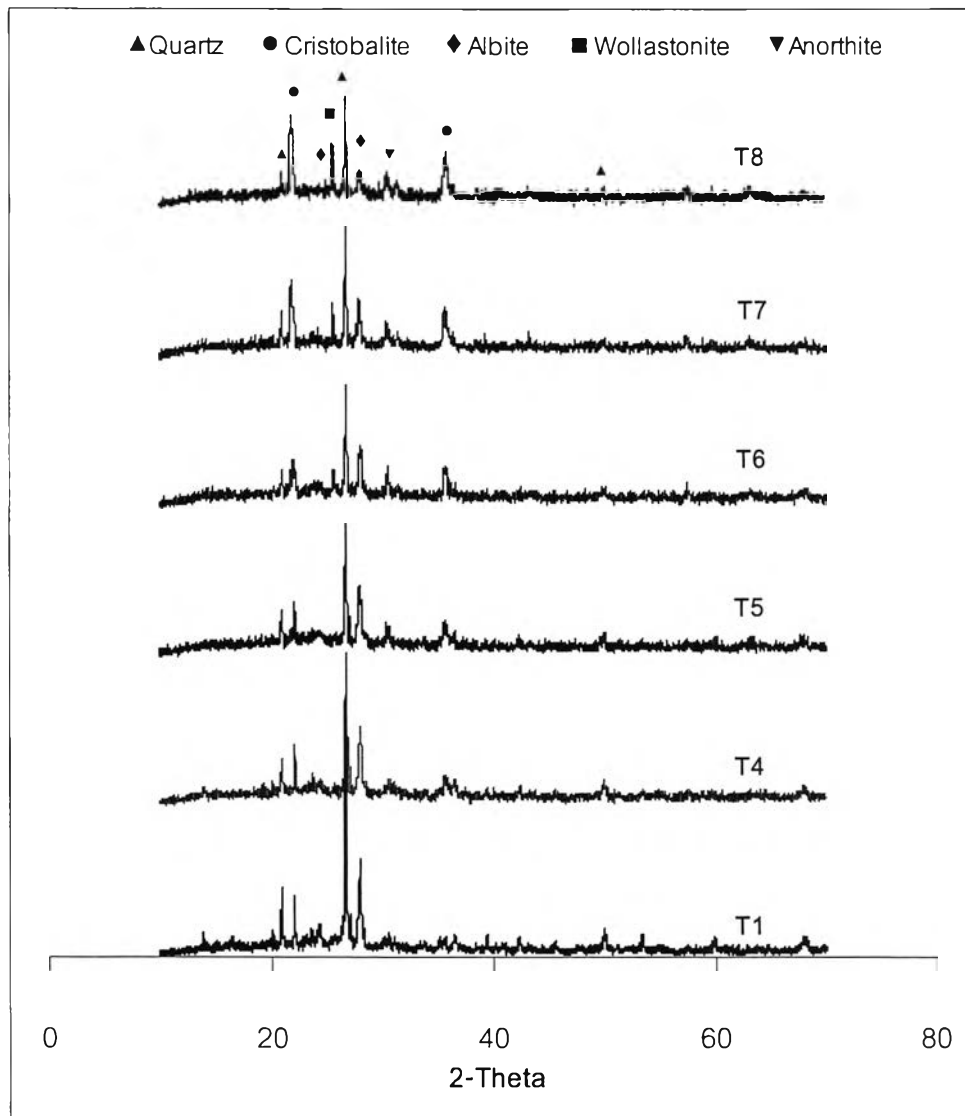


Fig 4.9 XRD pattern of specimens fired at 1125°C.

XRD patterns show the peak of quartz (SiO_2), cristobalite (SiO_2), albite ($\text{NaAlSi}_3\text{O}_8$) and anorthite ($\text{Ca}(\text{Al}_2\text{Si}_2\text{O}_8)$) in all specimens. There was decreased in the peak intensity of quartz and albite with an increase in amount of zinc waste while the intensity of cristobalite and anorthite peaks was increased.

The wollastonite (CaSiO_3) peak can be observed in specimens contained of 50% zinc waste or more (specimens T6, T7 and T8). An increase in zinc waste content in specimens led to an increase the ratio of CaO/SiO_2 . This resulted in higher intensity of wollastonite peak. Moreover, many auxiliary fluxes such as CaO , Na_2O , MgO and ZnO increased with an increase in percentage of waste. These oxides have a role in the transformation of quartz into cristobalite. The formation of albite was related to the amount of Al_2O_3 in composition. The intensity of albite decreased with a decrease in Al_2O_3 in specimen.

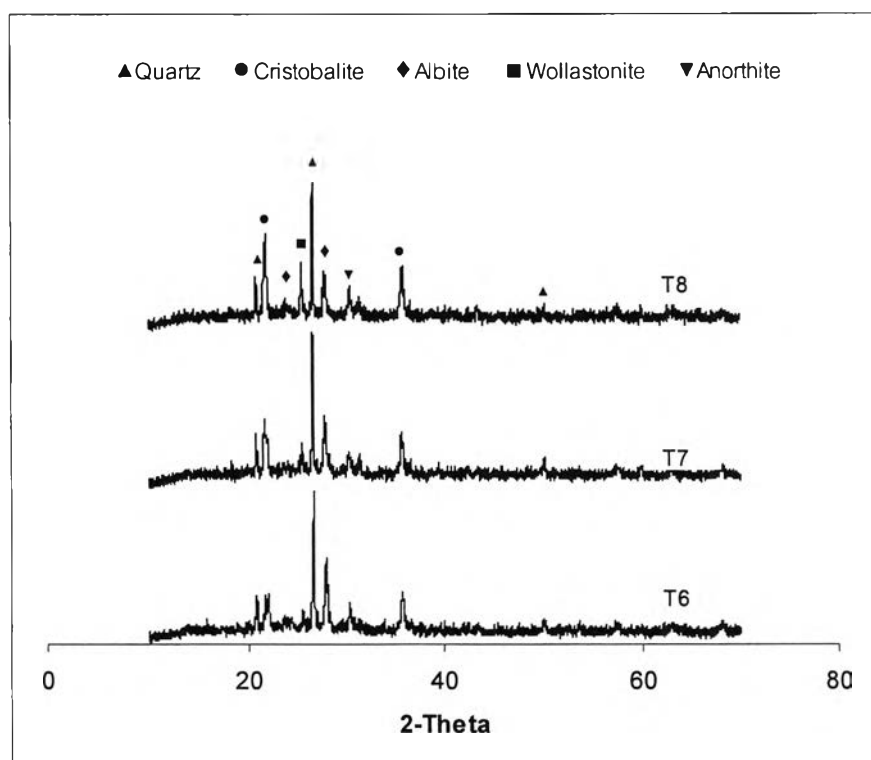


Fig 4.10 XRD pattern of specimens T6, T7 and T8 fired at 1100°C.

The effects of composition on phase formation were shown in Fig 4.10. It found that rising zinc waste percentage, there was a decrease in the peak intensity of quartz and albite while the intensity of cristobalite, anorthite and wollastonite peaks were increased.

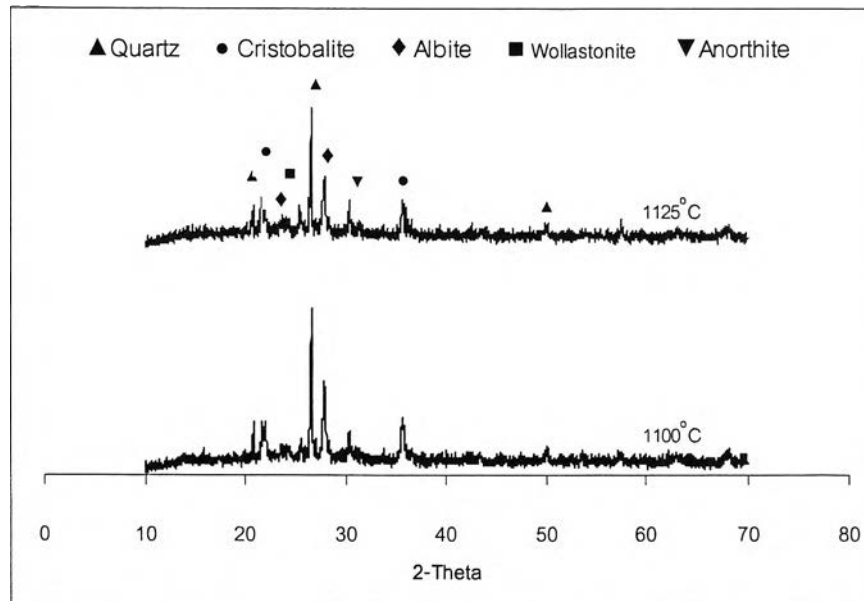


Fig 4.11 XRD pattern of specimens T6 fired at 1100°C and 1125°C.

The effects of firing temperatures on phase formation were also studied. Fig 4.11 shows the XRD pattern of specimens T6 fired at 1100°C and 1125°C. The presence of quartz (SiO_2), cristobalite (SiO_2), albite ($\text{NaAlSi}_3\text{O}_8$), anorthite ($\text{Ca}(\text{Al}_2\text{Si}_2\text{O}_8)$) and wollastonite (CaSiO_3) were found. At rising firing temperature from 1100°C to 1125°C, intensity of quartz and albite peaks decreased while intensity of cristobalite and wollastonite peaks increased.

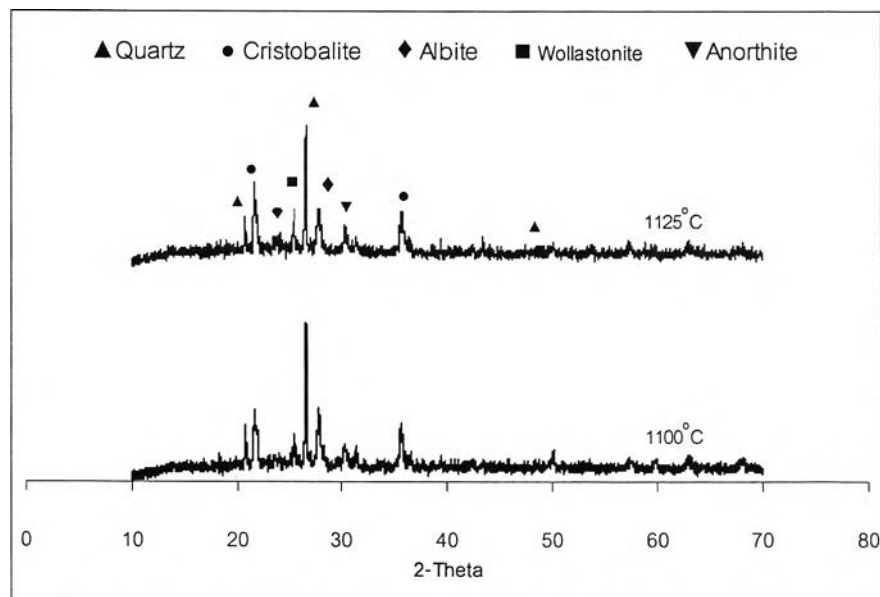


Fig 4.12 XRD pattern of specimens T7 fired at 1100°C and 1125°C

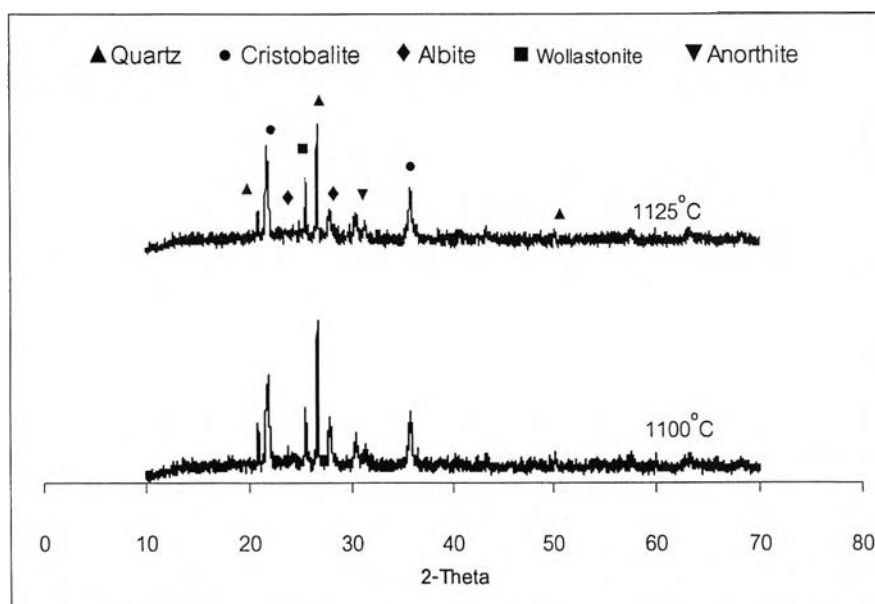


Fig 4.13 XRD pattern of specimens T8 fired at 1100°C and 1125°C

Similar to specimen T6, quartz (SiO_2), cristobalite (SiO_2), albite ($\text{NaAlSi}_3\text{O}_8$), anorthite ($\text{Ca}(\text{Al}_2\text{Si}_2\text{O}_8)$) and wollastonite (CaSiO_3) were observed in specimens T7 and T8 fired at 1100°C and 1125°C as shown in Fig 4.13 and Fig 4.14, respectively.

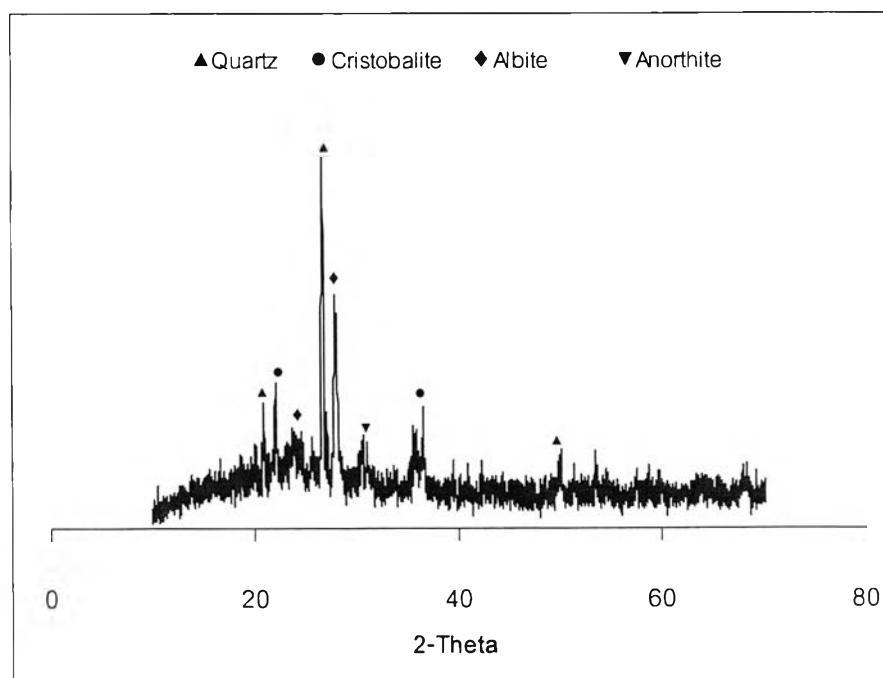


Fig 4.14 XRD pattern of specimens T4 fired at 1150°C.

Fig 4.14 shows the XRD pattern of specimens T4 at 1150°C. Quartz (SiO_2), cristobalite (SiO_2) and albite ($\text{NaAlSi}_3\text{O}_8$) were found as major phases with minor of anorthite ($\text{Ca}(\text{Al}_2\text{Si}_2\text{O}_8)$) phase. This is due to high content of SiO_2 , Al_2O_3 and Na_2O in this specimen.

4.2.1.4 Bending strength

Specimens T1, T4, T5, T6, T7 and T8 which has percent water absorption less than 5 % were selected to examine bending strength by using 3-point bending method.

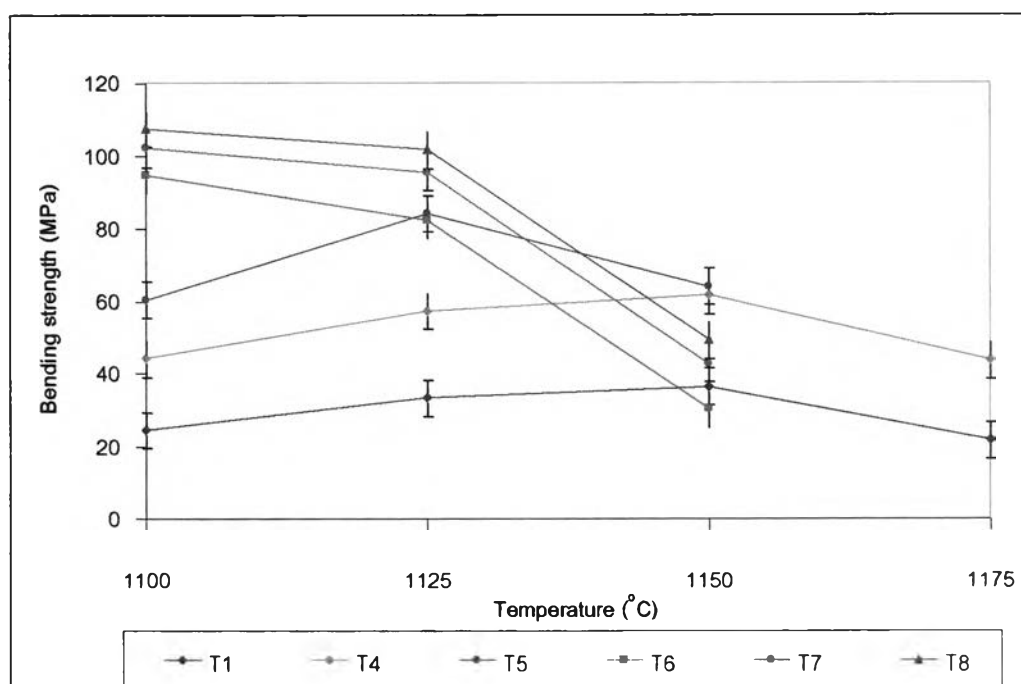


Fig 4.15 Three point bending strength of specimens

Bending strength of specimens fired at different temperatures was shown in Fig 4.15. Most of specimens gave the strength higher than the minimum limit of ISO 13006 (30 MPa for water absorption < 3%), except T1 fired at 1175°C was 21.55 MPa. The highest strength was found in specimen T8 fired at 1100°C. The strength of specimen T8 was 107.26 MPa. The bending strength of specimens depended on composition and firing temperature. The higher percentage of zinc waste in specimen gave the higher strength. Considering to firing temperature, at 1100°C, specimens

contained high percentage ($\geq 40\%$) of waste gave high strength. The maximum strengths were obtained in specimens T6, T7 and T8 at this temperature. At higher temperature (1125°C), strength of specimens contained high percentage ($\geq 40\%$) of waste decreased while bending strength of specimens contained lower percentage of waste increased. The bending strength of specimens contains lower percentage of waste slightly increased as a function temperature up to 1150°C . The strength of specimens was related to density and water absorption of specimens, high strength was obtained in specimen with high density and low water absorption. Those specimens which gave high strength (T6, T7 and T8) presence of wollastonite phase. Strength was improved by fiber structure of wollastonite. In addition, the presence of wollastonite was observed high strength in specimen. This suggested that this phase has an influence on the strength of the specimen.

4.2.1.5 Abrasive resistance

Abrasive resistance of specimens were tested by following standard of ISO 10545-6, the maximum limit of deep abrasive resistance was 175 mm^3 for unglazed tiles with water absorption less than 0.5% [27]. Deep abrasive resistances of specimens are shown in Table 4.2. Most of specimens shown abrasive resistance lower than the standard, except abrasive resistance of T8 was 184 mm^3 .

Table 4.2 Deep abrasive of specimens

Specimens		Volume (mm^3)
1100°C	T6	116
	T7	147
	T8	184
1125°C	T5	131
	T6	156
	T7	139
1150°C	T4	156

4.2.1.6 Chemical resistance

Chemical resistance of specimens was examined by ASTM C650 as shown in Table 4.3.

Table 4.3 Chemical resistance of specimens

Specimens		Phase	Test		
			HCl	KOH	HB pencil
1100°C	T6	Q, C, Al, An, W	X	√	√
	T7	Q, C, Al, An, W	X	X	√
	T8	Q, C, Al, An, W	√	√	√
1125°C	T5	Q, C, Al, An	√	√	√
	T6	Q, C, Al, An, W	√	√	√
	T7	Q, C, Al, An, W	X	√	√
1150°C	T4	Q, C, Al, An	√	√	√

note: X = specimen did not passed chemical testing.

√ = specimen passed chemical testing.

Specimen T6 fired at 1100°C showed poor in acid resistance while T7 fired at 1100°C poor in both acid and base resistance. The chemical resistance of specimens T6 and T7 were improved after firing at higher temperature; T6 passed in both acid and base resistance and T7 passed acid resistance.

According to XRD pattern, intensity of wollastonite peak in specimens T6 and T7 at 1125°C higher than 1100°C so it was noticeable that wollastonite is a factor to improve the chemical resistance of specimens.

These results show that most of the specimens show good resistance at any temperature.

4.2.1.7 Toxic leaching

Since zinc waste contained significant amount of toxic heavy metal that was lead (Pb), therefore it was very important to examine the Pb leaching. In Thailand,

there is no regular standard of heavy metal leaching thus the USA regulatory limit was selected to use as standard in this research.

Table 4.4 Pb leaching of specimens

Specimens		Phase	Pb release (ppm)
1100°C	T6	Q, C, Al, An, W	1.511
	T7	Q, C, Al, An, W	6.665
	T8	Q, C, Al, An, W	4.206
1125°C	T5	Q, C, Al, An	0.629
	T6	Q, C, Al, An, W	0.871
	T7	Q, C, Al, An, W	5.408
1150°C	T4	Q, C, Al, An	0.056

The released Pb was examined by using TCLP method. The released Pb were varied from 0.06 ppm - 6.67 ppm. It was found that the specimens without wollastonite phase gave the released Pb lower than the limits of USA (5 ppm), which were T6 fired at 1100°C and 1125°C, T8 at 1100°C, T5 fired at 1125°C and T4 fired at 1150°C.

It is note that the chemical resistance and leachability of specimen was improved after firing at higher temperature.

4.2.2 Characterization of glaze

4.2.2.1 Characterization of glaze using zinc waste as color stain

- Visual observation

Zinc waste was used as color stain in glossy glaze of stoneware, matt glaze for stoneware tile. The photographs of these glazes are shown in Fig 4.16 and Fig 4.17.

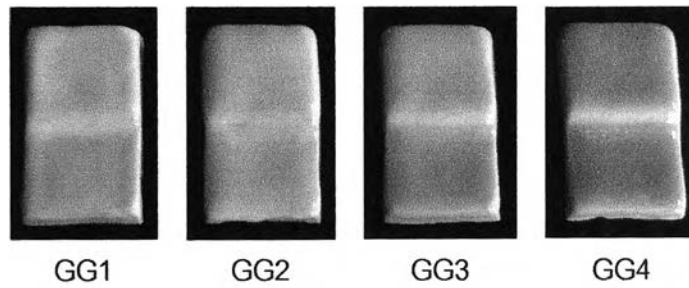


Fig 4.16 glossy glaze

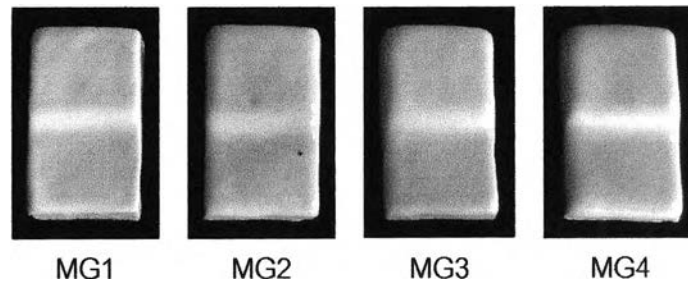


Fig 4.17 matt glaze

Color shade of glossy glaze and matte glaze were gradually change from white color to cream color which increased 5%, 10% and 15% zinc waste in glaze composition, respectively. However, the effect on glossy and matt appearance from percentage of zinc waste does not investigated.

The change of color depended on percentage of Fe_2O_3 . The higher percentage of Fe_2O_3 led to the darker color. As the percentage of zinc waste increased, percentage of Fe_2O_3 increased. Glossy glazes were gloss because it is composed of large amount of ZnO and matt glazes were matt because it is composed of large amount of Al_2O_3 .

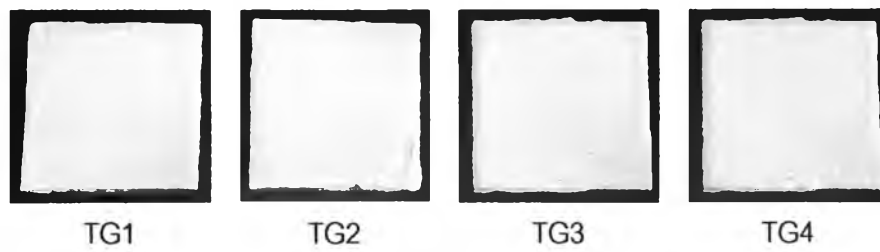


Fig 4.18 glaze stain for floor tiles

All glazes for tiles were yellow color caused by the consisting of Fe_2O_3 . Glazes TG1, TG2 and TG3 were gloss, while TG4 was matt.

4.2.2.2 Characterization of glaze base on frit from zinc waste

- Visual observation

Before quenching to form frit, the viscosity of the glasses was observed. It found that their viscosity were very low. This was because they contain high percentage of NaO, CaO and ZnO which were very active in reducing viscosity. The colors of frits were dark green due to Fe_2O_3 in the composition. The images of frits are shown in Fig 4.19.

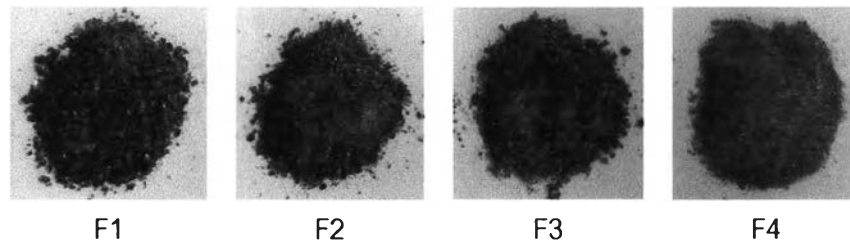


Fig 4.19 Image of frits

Fig 4.19 show the image of glazes base on frits from zinc waste for floor tiles and their physical properties are shown in Table 4.6.

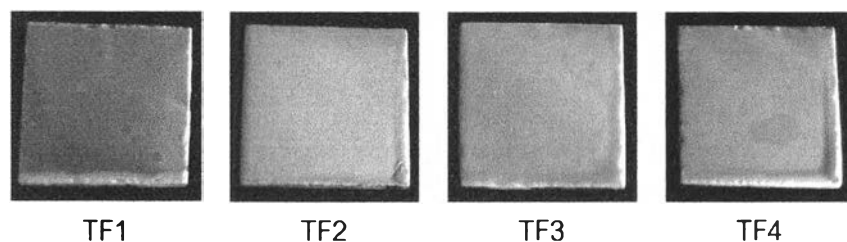


Fig 4.20 The image of glazes base on frits from zinc waste for floor tiles

All specimens were brown since they contain high percentage of Fe_2O_3 . TF1 and TF4 were glossy glaze while TF2 and TF3 were semi-matt glaze. TF2 contained low percentage of SiO_2 . Low percentage of SiO_2 gave low glassy phase, and as consequence they are low gloss. TF3 also contain low percentage of SiO_2 . Moreover, it contained high percentage of MgO that generated matt appearance.

Table4.5. The color and surface appearance of specimens.

Specimens	Color	Surface appearance
TF1	Brown	Gloss
TF2	Brown	Semi-matt
TF3	Brown	Semi-matt
TF4	Brown	Gloss

- Chemical resistance

Table4.6 show chemical resistance of glaze base on frit from zinc waste.

Table 4.6 Chemical resistance of glaze base on frit from zinc waste

Specimens	Test		
	HCl	KOH	HB pencil
TF1	√	√	√
TF2	√	√	√
TF3	√	√	√
TF4	X	X	√

note: X = specimen did not passed chemical testing.

√ = specimen passed chemical testing.

Considering to the chemical resistance, TF1, TF2 and TF3 showed good in both acid and base resistance. TF4 was poor in both acid and base resistance because it contains low percentage of B_2O_3 .